

Scheduling of UAV-assisted Millimeter Wave Communications for High-Speed Railway

Yibing Wang, Yong Niu, *Member, IEEE*, Hao Wu, Shiwen Mao, *Fellow, IEEE*, Bo Ai, *Fellow, IEEE*, Zhangdui Zhong, *Fellow, IEEE*, and Ning Wang

Abstract—To exploit richer spectrum resources for even better service quality, millimeter wave (mmWave) communication has been considered for high-speed railway (HSR) communication systems. In this paper, we focus on scheduling as many flows as possible while satisfying their QoS requirements. Due to interference, eavesdropping, or other problems, some flows may not be directly transmitted from the track-side BS. In this paper, we propose an UAV-assisted scheduling scheme which utilizes a UAV to serve as relay for such flows. The proposed scheme also utilize two mmWave bands, one for the BS links and the other for the UAV links. The proposed algorithm aims to maximize the number of flows with their QoS requirements satisfied. Simulations demonstrate that the proposed scheme achieves a superior performance on the number of completed flows and the system throughput over two baseline schemes.

Index Terms—High-speed railway (HSR), mmWave communications, quality of service (QoS), UAV-assisted communications.

I. INTRODUCTION

With the rapid development of high-speed railway (HSR) in recent years, there is a compelling need for high-quality broadband wireless access services for HSR. There is increasing demand to support data- and bandwidth intensive applications (e.g., multimedia applications) for HSR passengers. The current transmission rate requirement of each train cabin is about 37.5 Mbps according to a recent study, while may continue to grow and reach 0.5 ~ 5 Gbps in the future [1]. Obviously, these current transmission schemes cannot meet such increasing demands.

To this end, the millimeter wave (mmWave) band from 30 GHz to 300 GHz has abundant spectrum resources and can provide multi-gigabit transmission rates for bandwidth-intensive services, such as high-speed data transmission between devices (such as cameras, smartphones, tablets and laptops), compressed and uncompressed high-definition TV, real-time playback, wireless gaming, wireless personal area network, cellular access and wireless backhaul, etc. [2]–[5].

In this paper, we consider the mmWave communications between the HSR and the ground base station (BS). To

overcome the severe penetration loss of the train body shell, multiple mobile relays (MRs) are deployed on the rooftop of the train to provide better connections to the track-side BS. The passengers in the train communicates with the BS through radio access links, using the MRs as relays. MRs serve passengers via the APs which are installed in each carriage to avoid the penetration loss and frequent handover. Note that, the communications inside the train can use multiple radio access technologies, such as LTE or WiFi. In fact, the links between the MRs and the track-side BS are the main cause of the capacity bottleneck [6]. Thus, we focus our work on the mmWave communications between the BS and MRs.

In the typical scenario of mmWave HSR systems, there are a certain number of traffic flows to be transmitted. Each flow has its own minimum throughput requirement (i.e., the lowest transmission rate requirement), which is also referred to as its quality of service (QoS) requirement in this paper. Due to the diversity of applications, the QoS requirements of different flows are diverse. Furthermore, the mutual interference from concurrent link transmissions and the presence of eavesdroppers may cause some flows fail to be scheduled directly [7]. Therefore, we propose to deploy a UAV to relay the flows that cannot be directly transmitted from the BS to MRs under certain conditions. We present an UAV-assisted scheduling algorithm that exploits two mmWave bands (including one lower band for links from the BS and a higher band for links from the UAV) to achieve high system throughput. We also consider protecting the mmWave communications from potential eavesdroppers by enforcing the security capacity constraint. The main contributions of this paper are summarized as follows.

- To increase the network capacity of the HSR communication system and satisfy the needs of HSR passengers, we exploit the available spectrum resources of two mmWave frequency bands for the scheduled flows with diverse QoS requirements. The lower one of the two mmWave frequency bands is used for links from the BS, and the higher one is used for links from the UAV. Besides, we consider the existence of potential eavesdroppers, we determine whether a flow can be scheduled based on the security capacity to ensure its communication security.
- Due to interference, eavesdropping, or other problems, some flows cannot be directly scheduled from the BS to the MRs. To address this issue, we propose to use a UAV as a relay. With the assistance of the UAV, there is more flexibility for scheduling the flows. We formulate

Y. Wang, H. Wu, B. Ai and Z. Zhong are with the State Key Laboratory of Rail Traffic Control and Safety, Beijing Jiaotong University, Beijing 100044, China (Email: 18111034@bjtu.edu.cn).

Y. Niu is with the State Key Laboratory of Rail Traffic Control and Safety, Beijing Jiaotong University, Beijing 100044, China, and also with the National Mobile Communications Research Laboratory, Southeast University, Nanjing 211189, China (Email: niuy11@163.com).

S. mao is with the Department of Electrical and Computer Engineering, Auburn University, Auburn, AL 36849-5201, USA (Email: smao@ieee.org).

N. Wang is with the School of Information Engineering, Zhengzhou University, Zhengzhou 450001, China (Email: ienwang@zzu.edu.cn).

the problem of optimal scheduling as a nonlinear integer programming problem. Moreover, we propose a heuristic UAV-assisted scheduling algorithm to maximize the number of flows with their QoS requirements satisfied within a fixed time.

- We evaluate the proposed UAV-assisted scheduling scheme for the mmWave HSR network with simulations. Compared with two baseline schemes, the simulation results demonstrate that the proposed scheme achieves a superior performance on both the number of completed flows and the system throughput.

The remainder of this paper is organized as follows. In Section II, we review the related work. Section III presents the system model and assumptions. In Section IV, we formulate the optimal scheduling problem as a nonlinear integer programming problem. In Section V, we propose the relay decision algorithm and UAV-assisted scheduling algorithm. Section VI presents our simulation study of the proposed scheme. We conclude this paper in Section VII.

II. RELATED WORK

There are significant efforts on exploiting mmWave communications for augmented capacity for HSR systems. For the problem of flow forced interruption, utilizing other receivers/nodes as a one-hop or multihop relay to change the original transmission path is the most common solution [8]–[10]. In this paper, we do not use any original nodes to relay blocked flows, but use the UAV to create a new, high-altitude relay node. Due to the superiority of the UAV’s open location, superior relay effects can usually be achieved. Many prior works use alternative APs, which are densely deployed, to substitute direct paths from transmitter to receiver [11]–[14]. In this work, we adopt alternative APs in the HSR system, i.e., the MRs are deployed on top of the train to assist transmissions from the BS to passengers in the train.

There have been considerable prior works on scheduling in mmWave networks. Time division multiple access (TDMA) based schemes are commonly used in mmWave networks. Such schemes consider different types of link transmissions, including radio access, backhaul, and so on [15]–[18]. At present, many existing schemes aim to satisfy the QoS requirements of flows, where the scheduling scheme is designed under the premise of meeting the QoS requirement of each flow, and aiming to finally achieve different optimization goals [19], [20]. In this work, the goal is to develop a QoS-aware solution to schedule flows in HSR systems, which is assisted by an UAV relay. We consider the cooperation of two mmWave bands to achieve greater transmission capacity. We also consider the corresponding security measures against the communication security risks from potential eavesdroppers.

Recently, there have been a few studies on UAV-assisted relay networks [21]. The scheme of the optimal UAV placement is proposed for the single user or multiple users in the maritime communication, which can increase the capacity of wireless backhaul link between BS and UAV [22]. A cooperative secrecy transmission mechanism is presented for multiple UAV assisted relay selection to maximize the secrecy capacity [23].

In this paper, the transmission research is in HSR systems with the specific communication environment, and the completed link number and system throughput are maximized by scheduling link transmissions. UAV can serve as an energy source and provide RF energy for low power device-to-device (D2D) pairs [24]. Moreover, UAV enables the simultaneous wireless information and power transfer (SWIPT) system by jointly optimizing time switching-based relaying (TSR) and the optimization of its hovering location for better channel quality to maximize the network throughput [25]. These works usually assume the Rician fading channel as well as the line-of-sight (LoS) path between the UAV and each receiver [26]. To better model the actual channel state in HSR systems and to provide a better fit to real measurements observed in LoS scenarios, the κ - μ distribution was proposed in [27]–[30] as a general fading channel model where the Rician, Nakagami-m, and Rayleigh distributions are its special cases. In this paper, we adopt the α - β path loss model which is more in line with the path loss measurements in the HSR scenario. Besides, there are works which have studied the application of UAV-assisted communications in HSR system. Two UAV-assisted relaying transmission schemes are presented to allocate limited power for moving source and UAV, which are to save signaling overhead during the entire transfer process [31]. In this work, we proposed QoS-aware solution to maximize the number of scheduled flows. In addition, we allocate the time resource for two types of links and consider the cooperation of two mmWave bands for the links from BS to UAV and the links from UAV to MRs.

It is worth noting that these existing related works have not considered utilizing UAV to relay traffic flows which cannot be directly transmitted from the BS to MRs. In this paper, we integrate the dual-band cooperation of mmWave communications into the scheduling problem, aiming to maximize the number of scheduled flows. We also aim to satisfy the QoS requirements of each flow and avoid the potential risks caused by eavesdroppers. We will show through analysis and simulation that the proposed scheme can achieve a superior performance compared to the baseline schemes.

III. SYSTEM OVERVIEW

A. System Model

In this paper, we consider a single cell scenario of the mmWave HSR communication system, as shown in Fig. 1. A fixed BS is located beside the railway track, and a UAV is hovering above at a fixed position within the coverage of the track-side BS.

which are within the coverage range of the BS and UAV. The BS links are on frequency band f_1 , indicated by the black arrows in Fig. 1. The communications between the UAV and MRs are on frequency band f_2 , which are shown as red arrows in the figure. In addition, there is an eavesdropper, termed *Eva*, which is trying to overhear the communications. Without loss of generality, we assume *Eva* can only eavesdrop on the BS through frequency band f_1 .

There are F traffic flows between the BS and MRs, which need to be scheduled in the system. The UAV provides relay

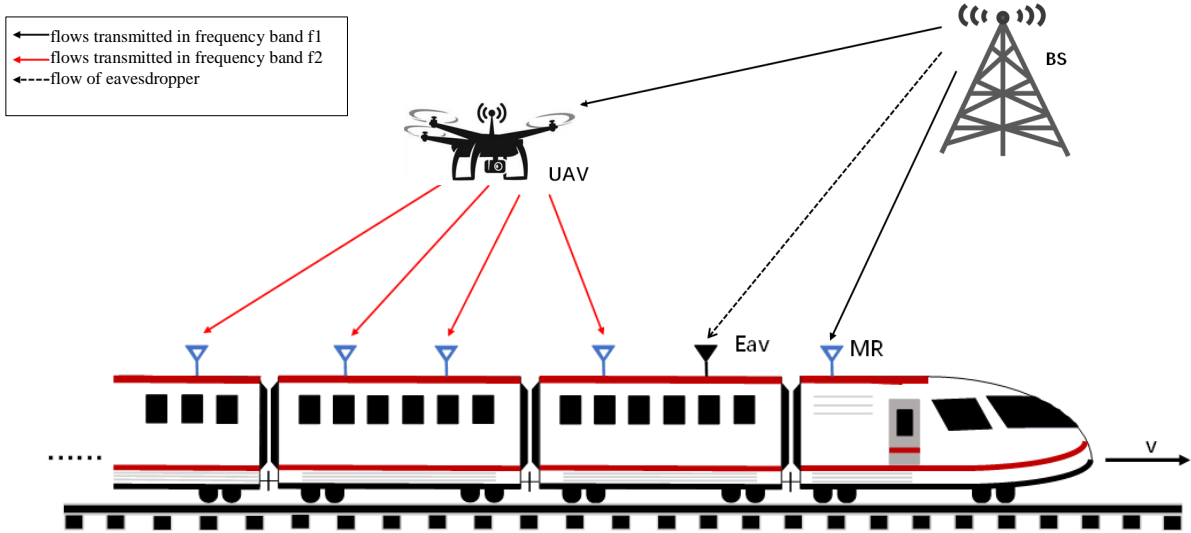


Fig. 1. The mmWave HSR communication system.

service in the air, thus each flow may be received from the BS directly or be relayed by the UAV for the destination MR. MRs can communicate with the track-side BS or the aerial UAV through radio access links. According to the selection of the transmission methods of the flows, some links are scheduled for transmission each time. In this paper, a link represents the actual connection of direct communications between two endpoints in the system.

In this paper, we consider the scenario where a train runs at a constant velocity $v = 300\text{km/h}$. In this case, the speed of the train is in line with reality. Although the train is moving at a high speed, the large bandwidth of mmWave allows the train to receive a large amount of data in a very short time. Therefore, the pressure of handover problem in high-speed railway communication can be greatly alleviated. We consider the downlink transmissions. The auxiliary transmission of UAV can effectively alleviate the link blockage problem caused by obstacles on the ground. All the devices in the system are assumed to operate in the half-duplex mode, i.e., they can only transmit or receive data at a time. Each MR is equipped with one steerable directional antenna, so it can only receive content from the BS or UAV at a time. The UAV is equipped with one directional antenna for receiving and N_{U_t} antennas for transmitting. The BS is equipped with N_{B_t} directional antennas for transmitting.

In the proposed system, time is divided into a series of non-overlapping super frames. Each super frame consists of a scheduling phase and a transmission phase. The scheduling phase is the time duration to collect link requests and their QoS requirements. The transmission phase consists of M equal time slots (TS). For clarity of exposition, we use TSs to measure the transmission time. For reliable transmissions, the control messages and BS requests can be transmitted with 4G technologies, including the source/destination information and the QoS requirements of each link [32]. The proposed scheduler is to allow multiple links be transmitted concurrently

using spatial-time division multiple access (STDMA) [33].

B. Antenna Model

As in prior works, directional antenna is necessary for mmWave communications [34]. We assume that the BS and UAV are both equipped with multiple directional antennas, which means they can send to multiple links simultaneously. However, each MR can receive from only the BS or UAV at a time. We adopt multiple antennas to form multiple directional beams at the BS and UAV for transmitting multiple data flows simultaneously [35]. The maximum numbers of beams formed simultaneously at the BS and UAV are limited by the numbers of theirs equipped transmitting antennas.

In this paper, we adopt the realistic directional antenna model which is mentioned in [36]. All directional antennas can steer their beams for the maximum directivity gain [37], [38]. The perfect beam alignment for the desired link has the maximum directivity antenna gain of G_0 . The antenna model can be expressed as

$$G_a(\theta) = \begin{cases} G_0 - 3.01 \cdot \left(\frac{2\theta}{\theta_{-3dB}}\right)^2, & 0^\circ \leq \theta \leq \theta_{ml}/2 \\ G_{sl}, & \theta_{ml}/2 \leq \theta \leq 180^\circ \end{cases} \quad (1)$$

where θ is an angle within the range $[0^\circ, 180^\circ]$. G_0 is the maximum antenna gain, $G_0 = 10 \log(1.6162 \sin(\theta_{-3dB}/2))^2$. θ_{-3dB} is the angle of the half-power beamwidth. θ_{ml} is the main lobe width, $\theta_{ml} = 2.6 \cdot \theta_{-3dB}$. G_{sl} is the sidelobe gain, $G_{sl} = -0.4111 \log(\theta_{-3dB}) - 10.579$.

The directional antenna model is for the antenna gain calculations of the links.

C. Transmission Model

The directional path loss in the target environment is studied via the impacts of antenna beam and propagation conditions. After evaluating the different existing models, the α - β model is selected as the path loss model for quantitative analysis

in this work [39]. For a link i , the path loss between its transmitter t_i and its receiver r_i is

$$PL(d_{t_i r_i}) = \alpha + 10\beta \log_{10}(d_{t_i r_i}) + X_\sigma, \quad (2)$$

where α and β are constants, $d_{t_i r_i}$ is the distance between t_i and r_i , and X_σ is a zero mean Gaussian random variable with a standard deviation σ .

Compared with line-of-sight (LOS) transmissions, non-line-of-sight (NLOS) transmissions suffer from much higher attenuation in the mmWave band [40]. Therefore we only consider the directional LOS links. For a link i , the received signal power at receiver r_i from transmitter t_i is

$$P_r(i, i) = G_{t_i} + G_{r_i} + Pt_i - PL(d_{t_i r_i}), \quad (3)$$

where G_{t_i} is the transmitter antenna gain of link i , G_{r_i} is the receiver antenna gain of link i , Pt_i is the transmit power at the transmitter of link i , and $PL(d_{t_i r_i})$ is calculated by (2).

Since we allow multiple links transmit concurrently by the STDMA transmission scheme, there is mutual interference between concurrent links using the same frequency band. For co-band concurrent links i and j , the interference at r_i from t_j can be calculated as

$$I_{ji} = G_{t_j} + G_{r_i} + Pt_j - PL(d_{t_j r_i}), \quad (4)$$

where G_{t_j} is the antenna gain at the transmitter of link j , G_{r_i} is the antenna gain at the receiver of link j , which is calculated as in (1), Pt_j is the transmit power at the transmitter of link j , and $PL(d_{t_j r_i})$ is calculated by (2).

According to Shannon's formula, the transmission rate of link i is given by

$$R_i = \eta W_i \log_2 \left(1 + \frac{P_r(i, i)}{N_0 W_i + \sum_{j \neq i} I_{ji}} \right), \quad (5)$$

where η describes the efficiency of the transceiver design, which is in the range of $(0, 1)$; W_i is the transmission bandwidth of link i ; and N_0 is the one-sided power spectra density of the white Gaussian noise.

We denote R_i^t as the actual transmit rate of link i in time slot t , which is calculated by (5). Then the achieved throughput of link i in this time slot can be obtained as

$$q_i^a = \frac{\sum_{t=1}^M R_i^t \cdot \Delta T}{T_s + M \Delta T}, \quad (6)$$

where T_s is the duration of the scheduling phase, and ΔT is the duration of each TS. The denominator in (6) is the duration of a super frame.

D. Secrecy Capacity Model

In this paper, we consider the existence of an eavesdropper, which can overhear the BS transmissions on frequency band f_1 . It is important to ensure secure communications and prevent information leakage. The secrecy capacity, an important physical layer security performance metric, is adopted to determine the feasibility of the schedule scheme in this work. Let C_M and C_E denote the Shannon capacities of the main

channel ($C_M = R_i$ if link i is attacked) and the eavesdropping channel, respectively. The secrecy capacity is given by [41]

$$C_S = C_M - C_E, \quad (7)$$

where C_M and C_E are both calculated by (5).

The position of the eavesdropper is constantly changing with the train moving. But the eavesdropper is fixed in a certain position of the train and is stationary relative to the train. Hence, compared with other randomly moving eavesdroppers, the location of the eavesdropper in this case is easier to estimate. The eavesdropper is not completely passive, and sends eavesdropping messages to the unknown receiver. The train is slow when it starts to run and can be regarded as stationary. At this time, we adopt the angle of arrival (AOA) positioning method to determine the specific location of the eavesdropper on the train [42]. The BS and MRs detect the signals sent by the eavesdropper to obtain the angles of incidences. Then the location of the eavesdropper can be determined by these angles of incidences. However, determination of the eavesdropper location facilitates the calculation of the security capacity.

IV. PROBLEM FORMULATION AND ANALYSIS

A. Problem Formulation

In this paper, the goal is to accommodate as many flows as possible through effective scheduling. In fact, different flows carry different types of service. Thus each flow f has its QoS requirement q_f in the form of its required minimum throughput. We define a binary variable δ_f to indicate whether flow f is scheduled successfully. If that is the case, we have $\delta_f = 1$; otherwise, $\delta_f = 0$. Let there be F flows. Then the objective function of the scheduler is given by

$$\max \sum_{i=1}^F \delta_f. \quad (8)$$

For link i , a binary variable a_i^t is defined to indicate whether the link is scheduled for transmission in time slot t . If so, $a_i^t = 1$; otherwise, $a_i^t = 0$. For the links generated from relayed flows, they are all transmitted to or received from the UAV. The following constraint enforces the half-duplex transmission condition.

$$a_i^t + a_j^t \leq 1, \quad \text{if } t_i = r_j \text{ or } r_i = t_j. \quad (9)$$

The constraint means the link to the UAV and the link from the UAV can't be scheduled concurrently. Each MR and the UAV can only receive a single link at a time. In other words, the receivers of any two concurrent links i and j must be different. Thus, we have the following constraint.

$$r_i \neq r_j, \quad \text{if } a_i^t = 1 \text{ and } a_j^t = 1. \quad (10)$$

Each link i has its QoS requirement q_i . The actual achieved throughput of each flow must satisfy its QoS requirement. For link i , the QoS constraint is as follows.

$$q_i^a = \frac{\sum_{t=1}^M R_i^t \cdot \Delta T}{T_s + M \Delta T} \geq q_i. \quad (11)$$

Regardless of whether it be the BS or UAV, the numbers of links can be simultaneously transmitted are limited by the

numbers of its transmit antennas. In time slot t , the set of links transmitted from the BS is defined as S_B^t , and the set of links transmitted from the UAV is defined as S_U^t . Then we have the following hardware constraint.

$$\sum_{i \in S_B^t} a_i^t \leq |N_{B_t}|, \text{ and } \sum_{j \in S_U^t} a_j^t \leq |N_{U_t}|. \quad (12)$$

Some flows are relayed by the UAV and then forwarded to the target MRs. The total throughput of the links transmitted from the BS is larger than the sum throughput of the links transmitted from the UAV.

$$\sum_{i \in \sum_{t=1}^T S_B^t} q_i^a \geq \sum_{j \in \sum_{t=1}^T S_U^t} q_j^a, \quad \tau \leq M, \quad (13)$$

where q_i^a and q_j^a are calculated as in (6).

Due to the existence of an eavesdropper, the confidentiality of transmissions must be guaranteed. The eavesdropping channel between a legitimate pair is a degraded version of the main channel [41]. In time slot t , the main channel capacity and the eavesdropping channel capacity of link i are denoted by C_M^i and C_E^i , with the following constraint [43].

$$C_E^i < 0.1 \cdot C_M^i, \quad i \in S_B^t, \quad (14)$$

The problem of maximizing the amount of scheduled flows in in each time slot can be formulated as follows.

$$\begin{aligned} \text{(P1) } \max \quad & \sum_{i=1}^F \delta_f, \\ \text{s.t. } \quad & (9) - (14). \end{aligned} \quad (15)$$

It can be seen that Problem P1 is a nonlinear integer programming problem. There are also complex nonlinear terms in the constraints. The problem is actually NP-hard [19], [44]. Thus, we aim to develop heuristic algorithms to obtain competitive solutions with low computational complexity.

V. THE UAV-ASSISTED SCHEDULING SCHEME

In this section, we propose an UAV-assisted scheduling scheme. With this scheme, each flow can choose from two transmission methods: one is to directly transmit from the BS to the target MR, and the other is to use the UAV as a relay. The proposed scheme first determines the transmission method for each flow and then schedules the links to transmit, aiming to maximize the number of scheduled flows.

A. The Relay Decision Algorithm

The relay decisions of the flows are based on their QoS requirements and the transmission efficiency. The flows that need to be scheduled are determined based on the transmitter-receiver ranges and their QoS requirements. Then we schedule the flows in each time slot for transmission.

We first consider whether the QoS requirements of the flows can be satisfied. Then we make a selection for each flow between being directly transmitted and being relayed. The set of the links which select to be directly transmitted from BS to MR is defined as S_1 , and the set of the links relayed by the UAV is defined as S_2 .

For each flow f , if it is directly transmitted from the BS to MR in the f_1 band, then this decision will allow one link l_1 from BS to MR to be scheduled. The achieved throughput $q_{l_1}^a$ of this link is computed as in (6). If flow f is to be relayed by the UAV in the f_2 band, then there are two links l_2 and l_2' to be scheduled: one from the BS to UAV and the other from the UAV to MR. The achieved throughput of these two links, $q_{l_2}^a$ and $q_{l_2'}^a$, can be calculated by (6). Since it is uncertain which links are transmitted simultaneously, the above throughput calculated by (6) does not consider the interference from other links. We can judge whether the two decisions (relay and no relay) can successfully transmit the flows by comparing the calculated throughputs and the QoS requirements. For flow f , the choice between direct transmission and relayed transmission can be decided as follows.

- 1) If $\min\{q_{l_1}^a, q_{l_2}^a, q_{l_2'}^a\} \geq q_f$, flow f can be scheduled by both choices.
- 2) If $q_{l_1}^a \geq q_f$ and $\min\{q_{l_2}^a, q_{l_2'}^a\} < q_f$, flow f can only be directly transmitted from the BS.
- 3) If $q_{l_1}^a < q_f$ and $\min\{q_{l_2}^a, q_{l_2'}^a\} \geq q_f$, flow f need to be relayed by the UAV.
- 4) If $q_{l_1}^a < q_f$ and $\min\{q_{l_2}^a, q_{l_2'}^a\} < q_f$, flow f should be abandoned. It should not be considered in the later scheduling process.

Since the eavesdropper is stealthily listening on the BS transmissions in the f_1 frequency band, the confidentiality of transmission should be considered. The location of the UAV ensures that the BS-UAV links can satisfy constraint (14). Thus the flows relayed by the UAV are less likely of being eavesdropped. For flows which are directly transmitted from the BS in the f_1 frequency band, we judge whether a direct transmission is feasible by evaluating (14).

To further compare the two transmission choices, we make a preliminary estimation of the transmission time of all the flows in $S_{all} = S_1 \cup S_2$. The number of estimated time slots of flow f can be obtained as follows.

$$T_{ef} = \begin{cases} \frac{q_f}{R_{l_1} \Delta T} & \text{if } f \in S_1 \\ \frac{q_f}{R_{l_2} \Delta T} + \frac{q_f}{R_{l_2'} \Delta T} & \text{if } f \in S_2. \end{cases} \quad (16)$$

Here R_i is the estimate rate without considering other links' interference at this time. The remaining flows select a better transmission choice by comparing the number of TSs required by the schedule.

The relay decision algorithm is summarized in Algorithm 1. First, we remove the flows whose QoS requirements cannot be satisfied by either of the two transmission choices in Line 2. In addition to the flows in set $\mathbb{D}_{\mathcal{U}}$, the other flows are divided into three categories based on whether their QoS requirements can be satisfied under different transmission choices in Lines 5-24. In Lines 5-6, the flows with their QoS requirements satisfied by being relayed by the UAV are added to S_2 . In Lines 9-13, the transmission methods for the other flows are determined, with their QoS requirements satisfied by direct transmission from the BS and satisfying the secrecy capacity condition. And these flows will be put in S_1 , the set of flows to be directly transmitted from the BS. In Lines 14-24, flows whose QoS

Algorithm 1: The Transmission Method Selection Algorithm

Input: $S_{all}, S_1 = \emptyset, S_2 = \emptyset$, QoS requirements of flows, locations of the BS, UAV, eavesdropper and MRs

Output: S_1, S_2

```

1 Calculate  $q_{l_1}^a, q_{l_2}^a$  and  $q_{l_2'}^a$  for each flow;
2 Remove  $\mathbb{D}_3 = \{f | q_{l_1}^a < q_f \text{ and } \min\{q_{l_2}^a, q_{l_2'}^a\} < q_f\}$  from
    $S_{all}$ ;
3 if  $|S_{all}| \neq 0$  then
4   for flow  $f$  ( $1 \leq f \leq |S_{all}|$ ) do
5     if  $q_{l_1}^a < q_f$  and  $\min\{q_{l_2}^a, q_{l_2'}^a\} \geq q_f$  then
6        $S_2 = S_2 \cup f$ ;
7        $S_{all} = S_{all} - f$ ;
8     else if  $q_{l_1}^a \geq q_f$  and  $\min\{q_{l_2}^a, q_{l_2'}^a\} < q_f$  then
9       if  $C_E^{l_1}$  can satisfy (14) then
10         $S_1 = S_1 \cup f$ ;
11         $S_{all} = S_{all} - f$ ;
12      else
13         $S_{all} = S_{all} - f$ ;
14      else if  $\min\{q_{l_1}^a, q_{l_2}^a, q_{l_2'}^a\} \geq q_f$  then
15        if  $C_E^{l_1}$  can't satisfy (14) then
16           $S_2 = S_2 \cup f$ ;
17           $S_{all} = S_{all} - f$ ;
18        else
19          if  $\frac{q_f}{R_{l_1} \Delta T} \leq (\frac{q_f}{R_{l_2} \Delta T} + \frac{q_f}{R_{l_2'} \Delta T})$  then
20             $S_1 = S_1 \cup f$ ;
21             $S_{all} = S_{all} - f$ ;
22          else
23             $S_2 = S_2 \cup f$ ;
24             $S_{all} = S_{all} - f$ ;

```

requirements can be satisfied by both transmission methods will be divided into three categories according to the secrecy capacity condition and transmission efficiency. If the secrecy capacity condition cannot be satisfied, it will be put in the set of flows relayed by the UAV, as in Lines 15-16. Finally, the remaining flows select their transmission methods by comparing the required transmission time of different choices as in Lines 19-24.

For the complexity of the transmission method selection algorithm, the number of the iterations of the outer `for` loop in Line 3 is $|S_{all}|$, where $|S_{all}|$ in the worst case is $\mathcal{O}(F)$. Hence, the computational complexity of the algorithm is $\mathcal{O}(F)$.

B. The UAV-assisted Scheduling Algorithm

Next we present a transmission scheduling algorithm. This scheduling algorithm is developed on the basis of the above transmission method selection algorithm.

We select the appropriate links for transmission in each TS based on the principle of maximizing the number of transmitted flows. For ease of exposition, we first introduce the simultaneous transmission requirements of links and the priority of link scheduling. Regarding the contention among links, we consider the three cases as follows.

- 1) Due to half-duplex transmissions, the link from the BS to the UAV and the link from the UAV to an MR cannot be scheduled concurrently.
- 2) If the simultaneous transmissions of two links will cause at least one of them to fail to satisfy the QoS requirement, there is a conflict between the two links.
- 3) As stated in (14), the links transmitted from the BS in the f_1 frequency band that do not meet the safe capacity threshold will not be scheduled simultaneously with other links.

A flow f relayed by the UAV will require two links l_2 and l_2' to be scheduled, i.e., l_2 from the BS to UAV and l_2' from the UAV to MR. We define the set of links scheduled in the f_1 band as S_{f_1} , and the set of links scheduled in the f_2 band as S_{f_2} . Link l_2 should be scheduled before l_2' . Thus we first schedule link $l_2 \in S_{f_1}$, and then link l_2' is generated in S_{f_2} to wait for being scheduled.

Then we consider the transmit order of the links in S_{f_1} or S_{f_2} . A parameter is defined to prioritize the scheduling order of the links, which is the inverse of a link's number of required TSs in a frame to satisfy its QoS requirement. For link i which is generated from flow f , the priority value is given by

$$\varpi_i = \frac{R_i \Delta t}{q_f (T_s + M \Delta t)}. \quad (17)$$

In fact, the less time the transmissions consume, the more flows can be completed in a fixed time interval. Prioritizing the flows that need fewer TSs can transmit more flows in a frame. Therefore, we calculate the priority values of links in S_{f_1} and S_{f_2} as (17), and then transmit the links in the descending order in the scheduling process. Since there are always new links joining S_{f_2} , the scheduling order of the links in the set needs to be frequently updated.

We define the set of the links which are to be transmitted from the BS to UAV as S_{BU} , and a parameter N_f is used to indicate the number of completed flows. The QoS-aware scheduling algorithm is summarized in Algorithm 2. First, the input and output of the algorithm are specified. Then, we configure sets S_{f_1} and S_{BU} in Lines 1-2. In Lines 7-14, we find the links in S_{f_1} that can be scheduled simultaneously with other selected transmitted links. In Lines 15-22, the simultaneous scheduled links in S_{f_2} are determined. In Lines 23-40, we obtain the remaining throughput demands of all the scheduled links after this time slot, and examine whether there are flows which have finished transmission in this TS.

The outer `for` loop of the scheduling algorithm has $\mathcal{O}(M)$ iterations. The `for` loop in Line 8 has $|S_{f_1}|$ iterations, and $|S_{f_1}|$ in the worst case is $\mathcal{O}(F)$. The `for` loop in Line 18 has $|S_{f_2}|$ iterations with the worst case value $\mathcal{O}(F)$. Moreover, the `for` loop in Line 23 has $|SS|$ iterations, and its worst case value is also $\mathcal{O}(F)$. The `for` loops in Line 8, Line 18 and Line 23 are parallel. Therefore, the complexity of the QoS-based scheduling algorithm is $\mathcal{O}(MF)$. Such low complexity of the algorithm makes it suitable for practical implementation.

VI. PERFORMANCE EVALUATION

In this section, we evaluate the performance of the UAV-assisted scheduling algorithm. The flow transmissions of the

Algorithm 2: The UAV-assisted Scheduling Algorithm

Input: $S_1, S_2, S_{BU} = \emptyset, S_{f_1} = S_1, S_{f_2} = \emptyset, N_f = 0, SS = \emptyset, \alpha = 0, n_{B_t} = 0, n_{U_t} = 0, q_f$

Output: N_f

- 1 **for** flow $f \in S_2$ **do**
- 2 $S_{f_1} = S_{f_1} \cup l_2$ (link l_2 is generated by flow $f \in S_2$ scheduling);
- 3 $S_{BU} = S_{BU} \cup l_2$;
- 4 Calculate the priority values of the links in S_{f_1} ;
- 5 Sort the links in S_{f_1} in increasing order by priority value;
- 6 **for** time slot t ($1 \leq t \leq M$) **do**
- 7 **if** $|S_{f_1} \cup S_{f_2}| \neq 0$ **then**
- 8 **if** $|S_{f_1}| \neq 0$ **then**
- 9 **for** link i ($1 \leq i \leq |S_{f_1}|$) **do**
- 10 **if** $n_{B_t} < N_{B_t}$ **then**
- 11 **if** i has no contention with the link(s) in SS **then**
- 12 $SS = SS \cup i$;
- 13 $n_{B_t} = n_{B_t} + 1$;
- 14 **if** $i \in S_{BU}$ **then**
- 15 $\alpha = 1$;
- 16 $S_{f_2} = S_{f_2} \cup l'_2$ (link l'_2 is generated by flow $f \in S_2$ scheduling);
- 17 **if** $\alpha = 0 \& |S_{f_2}| \neq 0$ **then**
- 18 calculate the priority values of the links in S_{f_2} ;
- 19 Sort the links in S_{f_2} in increasing order by priority value;
- 20 **for** link i' ($1 \leq i' \leq |S_{f_2}|$) **do**
- 21 **if** $n_{U_t} < N_{U_t}$ **then**
- 22 **if** i' has no contention with the link(s) in SS **then**
- 23 $SS = SS \cup i'$;
- 24 $n_{U_t} = n_{U_t} + 1$;
- 25 **for** each link $j \in SS$ **do**
- 26 Calculate the rate R_j in the current time slot;
- 27 Calculate the remaining throughput demand of j ,
- 28 $q_j = q_j * (T_s + M \cdot \Delta t) - R_j^\delta * \Delta t$ (q_j can obtain from the QoS requirement of the corresponding flow);
- 29 **if** $q_j \leq 0$ **then**
- 30 $SS = SS - j$;
- 31 **if** $j \in S_{f_1}$ **then**
- 32 $S_{f_1} = S_{f_1} - j$;
- 33 $n_{B_t} = n_{B_t} - 1$;
- 34 **if** $j \in S_{BU}$ **then**
- 35 $\alpha = 0$;
- 36 $S_{BU} = S_{BU} - j$;
- 37 **else**
- 38 $N_f = N_f + 1$;
- 39 **else**
- 40 $S_{f_2} = S_{f_2} - j$;
- 41 $n_{U_t} = n_{U_t} - 1$;
- 42 $N_f = N_f + 1$;

scheme involve two bands: f_1 in the 28GHz band and f_2 in the 60GHz band. We also compare the performance of the proposed scheme with several existing baseline schemes.

TABLE I
SIMULATION PARAMETERS

Parameter	Symbol	Value
carrier frequency 1	f_1	28 GHz
carrier frequency 2	f_2	60 GHz
28GHz bandwidth	W_1^{mm}	850 MHz
60GHz bandwidth	W_2^{mm}	1500 MHz
Height of BS	h_{BS}	10 m
Height of MR	h_{MR}	2.5 m
Height of UAV	h_{UAV}	100 m
Number of BS transmit antennas	N_{B_t}	3
Number of UAV transmit antennas	N_{U_t}	3
transceiver efficiency factor	η	0.5
background noise	N_0	-134dBm/MHz
slot time	Δt	18 μ s
beacon period	T_s	850 μ s
Maximum antenna gain	G_0	20dBi
Maximum attenuation of antenna model	A_m	26dB
Half-power beamwidth	θ_{-3dB}	15 $^\circ$

TABLE II
EXTRACTED PARAMETERS OF THE PATH LOSS MODEL FOR URBAN STRAIGHT ROUTE SCENARIOS

Straight	α		β		σ
	$d \leq 153.3$	$d > 153.3$	$d \leq 153.3$	$d > 153.3$	
Urban	108.75	42.34	-1.45	1.59	5.85

A. Simulation Setup

We consider the single cell scenario of the mmWave HSR system. There are 24 MRs which are evenly distributed on top of the train. The flows which need to be scheduled are all transmitted from the BS. Then the flows are generated by randomly selecting the receivers among all the MRs. The train has a total of eight cars with a total length of 200m. Three MRs are deployed in each car. One eavesdropper is randomly placed on top of the train. The BS and UAV can reach a communication range of hundreds of meters, and all the links in the system are transmitted within the allowable communication ranges of their transceivers. The number of flows which need to be transmitted between the BS and MRs is smaller than the number of MRs.

Since the MRs move at the high speed with the train, we need to update their location information periodically. We collect and update the location information of MRs every 2000 time slots in the process. During this period of time, the change distances of MRs do not exceed 3m, which does not affect the data transmissions.

Besides, each carriage of the train has 50-100 seats, then each MR has to deal with the data traffic requirements of 10-20 passengers at most. The flow of each MR request may be a combination of the traffic flows of multiple passengers. Thus, the QoS requirement values of scheduled flows fluctuates in a wide range. We assume that the QoS requirement of each flow is uniformly distributed between 10Mbps and 500Mbps. Other parameters are presented in Table I [14], [35], [39]. For the path loss model, the specific expression is given in (2) and the parameter settings are from [39], which are summarized in Table II.

For the performance evaluation study, the following performance metrics are used.

- Number of completed flows: the number of scheduled flows with their QoS requirements satisfied. If the QoS requirement cannot be met, the flow that has been scheduled will not be counted as a completed flow.
- System throughput: the total throughput of the entire network system. This metric is the sum of the average throughputs of all the flows carried in the network.
- Total amount of time slots: the total number of time slots used to transmit all the scheduled flows. The actual value of this metric must be smaller than the total number of TSs in the frame.

For comparison purpose, we implement the state-of-the-art QoS-aware Concurrent Scheme [17] and Maximum QoS-aware Independent Set (MQIS) based scheduling algorithm [19] as baseline schemes.

- QoS-aware Concurrent Scheme [17]: this is a concurrent scheduling scheme aiming to satisfy the QoS requirements of flows and to maximize the number of flows. If a flow cannot meet the current scheduling conditions, the scheme cannot relay the flow and has to give up scheduling it.
- MQIS [19]: this is the scheduling algorithm based on the concept of maximum QoS-aware independent set proposed in [19]. The algorithm divides flows into multiple independent sets. Only after all the flows in one set are scheduled transmitted, the flows in another set can begin to be scheduled.

B. Comparison with Existing Schemes

In Fig. 2, we plot the number of completed flows under different numbers of requested flows. The horizontal distance between the UAV and BS is set to $150m$, and the number of time slots is set to $8,000$. With the increased number of requested flows, we can see that the curves for the three schemes are all rising. The more requested flows in the HSR network, the more flows can complete their scheduling. For the proposed UAV-assisted scheduling scheme, some flows which cannot be directly transmitted from the BS can choose to be scheduled by UAV relaying. Therefore, the proposed scheme achieves a superior performance with respect to the number of completed flows compared with the other two schemes. When the number of flows is 18, the proposed scheme outperforms the QoS-aware concurrent scheme with a gain of 35.0% and MQIS with a gain of 32.4%.

In Fig. 3, we plot the system throughput under different numbers of requested flows. The horizontal distance between the UAV and BS and the number of time slots are the same as in Fig. 2. From the figure, we can see that the system throughput of the three schemes are all increasing with the increased number of requested flows. For each flow, our proposed scheme can decide whether to use UAV relaying according to the principle of transmission rate maximization. The proposed scheme achieves the largest system throughput among the three scheme. It can also relay some flows which cannot be directly transmitted from the BS. The QoS-aware scheme and MQIS have similar performance on the system throughput. When the number of requested flows is 18, the

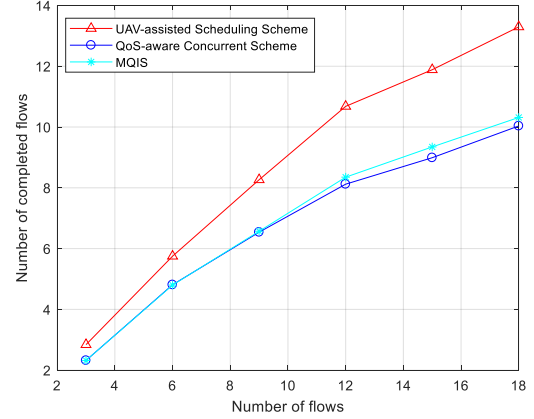


Fig. 2. Number of completed flows versus different numbers of requested flows.

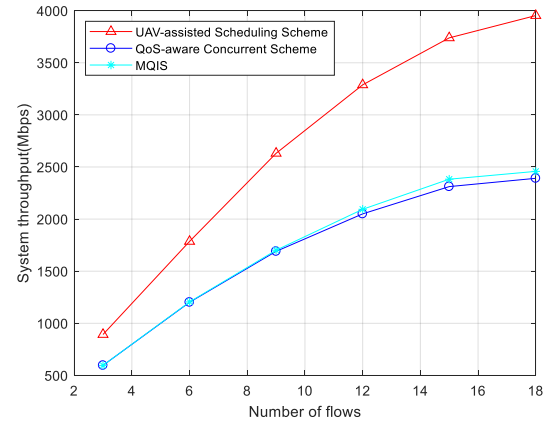


Fig. 3. System throughput versus different numbers of requested flows.

proposed UAV-assisted scheduling scheme outperforms the QoS-aware concurrent scheme with a gain of 64.6% and MQIS with a gain of 61.2%.

In Fig. 4, we plot the system throughput under different numbers of requested flows. The horizontal distance between the UAV and BS and the number of time slots remain the same as previous simulations. From this figure, we can see that the total number of slots of the three schemes are all increasing as more flows are requested. Although the proposed scheme can schedule the most flows among the three schemes, as shown in Fig. 2, it can be seen from Fig. 4 that the total numbers of time slots needed by the three schemes are very similar. This proves that the proposed UAV-assisted scheme has a superior performance on transmission efficiency compared with the QoS-aware concurrent scheme and MQIS.

In Fig. 5, we plot the number of completed flows under different numbers of time slots in each frame. The horizontal distance between the UAV and BS is set to $150m$, and the

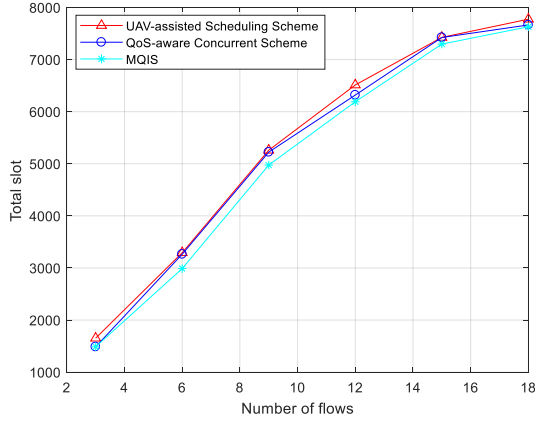


Fig. 4. Number of time slots versus different numbers of requested flows.

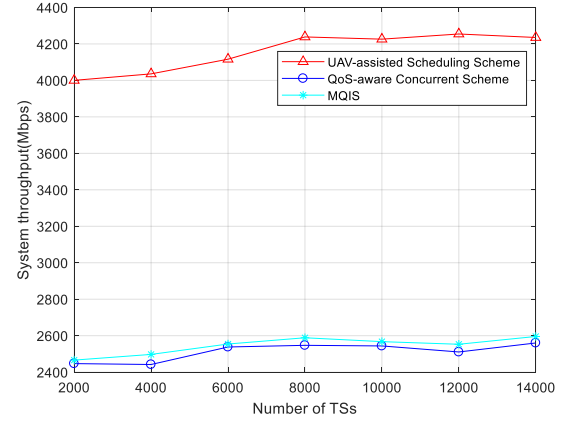


Fig. 6. System throughput versus different numbers of time slots.

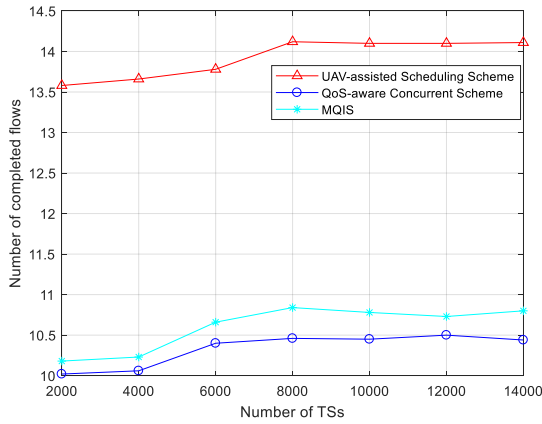


Fig. 5. Number of completed flows versus different numbers of time slots in each frame.

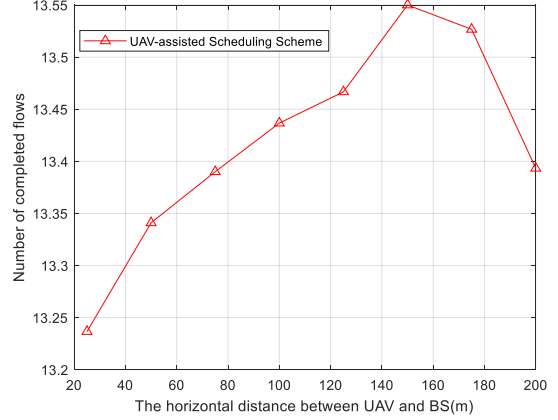


Fig. 7. Number of completed flows versus different horizontal distances between the UAV and BS.

number of requested flows is set to 18. When the number of time slots begin to increases, the curves of the three schemes are all rising. When the number of time slots increases to a certain value, the numbers of completed flows of three schemes are all becoming steady. Therefore, the number of time slots does not need to be increased to a very large value; an appropriate value of time slot number in each scheme can ensure a satisfactory performance.

In Fig. 6, we plot the system throughput under different numbers of time slots. The horizontal distance between UAV and BS and the number of requested flows are the same as that in Fig. 5. From the figure, we can see similar trends for the three schemes as in Fig. 5. With the increased number of time slots, we can see that the curves for the three schemes are all rising. The more time slots, the more system throughput can achieve during scheduling. The three curves start to stabilize when the number of slots is increased over 8,000. Hence, the number of TSs is set to 8,000 in the other simulations.

In Fig. 7, we plot the number of completed flows under different horizontal distances between UAV and BS, to demonstrate the impact of the UAV location on performance. The number of requested flows is set to 18, and the number of time slots is set to 8,000. With the increased horizontal UAV-BS distance, the number of completed flows increases first and then declines. Thus a suitable location of the UAV has a significant impact on the system performance. When UAV-BS distance is 150 m, the number of completed flows reaches the maximum value. Thus, the horizontal distance between the UAV and BS is set to 150 m in all the other simulations.

VII. CONCLUSIONS

In this paper, we considered the problem of scheduling flows with diverse QoS requirements in the scenario of mmWave HSR communications. To maximize the number of flows while satisfying their QoS requirements, we proposed the UAV-assisted scheduling scheme to deploy a UAV relay to assist

the scheduling of flows. Our simulation study showed that the proposed UAV-assisted scheme outperformed two baseline schemes on the number of completed flows, achievable system throughput, and transmission efficiency.

REFERENCES

- [1] B. Lannoo, D. Colle, M. Pickavet, and P. Demeester, "Radio-over-fiber-based solution to provide broadband Internet access to train passengers," *IEEE Commun. Mag.*, vol. 45, no. 2, pp. 56–62, Feb. 2007.
- [2] M. El-kashlan, T. Q. Duong, and H.-H. Chen, "Millimeter-wave communications for 5G: Fundamentals:Part I [Guest Editorial]," *IEEE Commun. Mag.*, vol. 52, no. 9, pp. 52–54, Sept. 2014.
- [3] S. Singh, R. Mudumbai, and U. Madhoo, "Distributed coordination with deaf neighbors: Efficient medium access for 60 GHz mesh networks," in *Proc. IEEE INFOCOM'10*, San Diego, CA, Mar. 2010, pp. 1–9.
- [4] C. Sum, Z. Lan, R. Funada, J. Wang, T. Baykas, M. A. Rahman, and H. Harada, "Virtual time-slot allocation scheme for throughput enhancement in a millimeter-wave multi-Gbps WPAN system," *IEEE J. Sel. Areas Commun.*, vol. 27, no. 8, pp. 1379–1389, Oct. 2009.
- [5] F. Gutierrez, S. Agarwal, K. Parrish, and T. S. Rappaport, "On-chip integrated antenna structures in CMOS for 60 GHz WPAN systems," *IEEE J. Selected Areas in Communications*, vol. 27, no. 8, pp. 1367–1378, Oct. 2009.
- [6] C. Zhang, P. Fan, K. Xiong, and P. Fan, "Optimal power allocation with delay constraint for signal transmission from a moving train to base stations in high-speed railway scenarios," *IEEE Trans. Veh. Technol.*, vol. 64, no. 12, pp. 5775–5788, Dec. 2015.
- [7] H. Song, X. Fang, and Y. Fang, "Millimeter-wave network architectures for future high-speed railway communications: Challenges and solutions," *IEEE Wireless Commun. Mag.*, vol. 23, no. 6, pp. 114–122, Dec. 2016.
- [8] J. Wang, R. V. Prasad, and I. G. Niemegeers, "Exploring multipath capacity for indoor 60 GHz radio networks," in *Proc. IEEE ICC'10*, Cape Town, South Africa, May 2010, pp. 1–6.
- [9] Y. Niu, W. Ding, H. Wu, Y. Li, X. Chen, B. Ai, and Z. Zhong, "Relay-assisted and QoS aware scheduling to overcome blockage in mmWave backhaul networks," *IEEE Trans. Veh. Technol.*, vol. 68, no. 2, pp. 1733–1744, Feb. 2019.
- [10] W. Kim, J. Song, and S. Baek, "Relay-assisted handover to overcome blockage in millimeter-wave networks," in *Proc. IEEE PIMRC'17*, Montreal, Canada, Oct. 2017, pp. 1–5.
- [11] I. K. Jain, R. P. Kumar, and S. S. Panwar, "Driven by capacity or blockage? A millimeter wave blockage analysis," in *Proc. ITC'18*, Vienna, Austria, Sept. 2018, pp. 153–159.
- [12] X. Zhang, S. Zhou, X. Wang, Z. Niu, X. Lin, D. Zhu, and M. Lei, "Improving network throughput in 60GHz WLANs via multi-AP diversity," in *Proc. IEEE ICC'12*, Ottawa, Canada, June 2012, pp. 4803–4807.
- [13] D. D. Ramírez, L. Huang, Y. Wang, and B. Aazhang, "On opportunistic mmWave networks with blockage," *IEEE J. Sel. Areas Commun.*, vol. 35, no. 9, pp. 2137–2147, Sept. 2017.
- [14] M. Gao, B. Ai, Y. Niu, W. Wu, P. Yang, F. Lyu, and X. Shen, "Efficient hybrid beamforming with anti-blockage design for high-speed railway communications," *IEEE Trans. Veh. Technol.*, vol. 69, no. 9, pp. 9643–9655, Sept. 2020.
- [15] R. Taori, and A. Sridharan, "Point-to-multipoint in-band mmWave backhaul for 5G networks," *IEEE Commun. Mag.*, vol. 53, no. 1, pp. 195–201, Jan. 2015.
- [16] Y. Niu, C. Gao, Y. Li, L. Su, D. Jin, and A. V. Vasilakos, "Exploiting device-to-device communications in joint scheduling of access and backhaul for mmWave small cells," *IEEE J. Sel. Areas Commun.*, vol. 33, no. 10, pp. 2052–2069, Oct. 2015.
- [17] W. Ding, Y. Niu, H. Wu, Y. Li, and Z. Zhong, "QoS-aware full-duplex concurrent scheduling for millimeter wave wireless backhaul networks," *IEEE Access J.*, vol. 6, pp. 25313–25322, Apr. 2018.
- [18] Z. He, S. Mao, S. Kompella, and A. Swami, "On link scheduling in dual-hop 60 GHz mmWave networks," *IEEE Trans. Veh. Technol.*, vol. 66, no. 12, pp. 11180–11192, Dec. 2017.
- [19] J. Qiao, L. X. Cai, X. Shen, and J. Mark, "STDMA-based scheduling algorithm for concurrent transmissions in directional millimeter wave networks," in *Proc. IEEE ICC'12*, Ottawa, Canada, June 2012, pp. 5221–5225.
- [20] Y. Zhu, Y. Niu, J. Li, D. O. Wu, Y. Li, and D. Jin, "QoS-aware scheduling for small cell millimeter wave mesh backhaul," in *Proc. IEEE ICC'16*, Kuala Lumpur, Malaysia, May 2016, pp. 1–6.
- [21] C. Zhan, H. Hu, Z. Liu, Z. Wang, and S. Mao, "Multi-UAV-enabled mobile edge computing for time-constrained IoT applications," *IEEE Internet of Things Journal*, to appear. DOI: 10.1109/JIOT.2021.3073208.
- [22] J. Zhang, F. Liang, B. Li, Z. Yang, Y. Wu and H. Zhu, "Placement optimization of caching UAV-assisted mobile relay maritime communication," *China Communications*, vol. 17, no. 8, pp. 209–219, Aug. 2020.
- [23] B. Ji, Y. Li, D. Cao, C. Li, S. Mumtaz, and D. Wang, "Secrecy Performance Analysis of UAV Assisted Relay Transmission for Cognitive Network With Energy Harvesting," *IEEE Transactions on Vehicular Technology*, vol. 69, no. 7, pp. 7404–7415, Jul. 2020.
- [24] H. Wang, J. Wang, G. Ding, L. Wang, T. A. Tsiftsis, and P. K. Sharma, "Resource allocation for energy harvesting-powered D2D communication underlying UAV-assisted networks," *IEEE Trans. Green Commun. Netw.*, vol. 2, no. 1, pp. 14–24, Mar. 2018.
- [25] M. Hua, C. Li, Y. Huang, and L. Yang, "Throughput maximization for UAV-enabled wireless power transfer in relaying system," in *Proc. WCSP'17*, Nanjing, China, Oct. 2017, pp. 1–5.
- [26] J. Zhang, L. Dai, Z. He, S. Jin, and X. Li, "Performance analysis of mixed-ADC massive MIMO systems over Rician fading channels," *IEEE J. Sel. Areas Commun.*, vol. 35, no. 6, pp. 1327–1338, June 2017.
- [27] B. Ji, Y. Li, S. chen, C. Han, C. Li, and H. Wen, "Secrecy Outage Analysis of UAV Assisted Relay and Antenna Selection for Cognitive Network Under Nakagami-m Channel," *IEEE Transactions on Cognitive Communications and Networking*, vol. 6, no. 3, pp. 904–914, Sep. 2020.
- [28] J. Zhang, X. Chen, K. P. Peppas, X. Li, and Y. Liu, "On high-order capacity statistics of spectrum aggregation systems over $\kappa - \mu$ and $\kappa - \mu$ shadowed fading channels," *IEEE Trans. Commun.*, vol. 65, no. 2, pp. 935–944, Feb. 2017.
- [29] J. Zhang, Z. Tan, H. Wang, Q. Huang, and L. Hanzo, "The effective throughput of MISO systems over $\kappa - \mu$ fading channels," *IEEE Trans. Veh. Technol.*, vol. 63, no. 2, pp. 943–947, Feb. 2014.
- [30] J. Zhang, M. Matthaiou, G. K. Karagiannidis, H. Wang, and Z. Tan, "Gallager's exponent analysis of STBC MIMO systems over $\eta - \mu$ and $\kappa - \mu$ fading channels," *IEEE Trans. Commun.*, vol. 61, no. 3, pp. 1028–1039, Mar. 2013.
- [31] J. Wu, L. Li and L. Du, "UAV-Assisted Relaying Transmission Design and Optimization for High-Speed Moving Sources," *IEEE Access*, vol. 8, pp. 195857–195869, Oct. 2020.
- [32] J. Qiao, X. S. Shen, J. W. Mark, Q. Shen, Y. He, and L. Lei, "Enabling device-to-device communications in millimeter-wave 5G cellular networks," *IEEE Commun. Mag.*, vol. 53, no. 1, pp. 209–215, Jan. 2015.
- [33] J. Qiao, L. X. Cai, and X. Shen, et. al., "Enabling multi-hop concurrent transmissions in 60 GHz wireless personal area networks," *IEEE Trans. Wireless Commun.*, vol. 10, no. 11, pp. 3824–3833, Nov. 2011.
- [34] Y. Azar et al., "28GHz propagation measurements for outdoor cellular communications using steerable beam antennas in New York City," in *Proc. IEEE ICC'13*, Budapest, Hungary, June 2013, pp. 5143–5147.
- [35] S. Pyun, H. Widiarti, Y. Kwon, D. Cho, and J. Son, "TDMA-based channel access scheme for V2I communication system using smart antenna," in *Proc. 2010 IEEE Vehicular Networking Conference*, Jersey City, NJ, Dec. 2010, pp. 209–214.
- [36] Q. Chen, X. Peng, J. Yang, and F. Chin, "Spatial reuse strategy in mmWave WPANs with directional antennas," in *Proc. IEEE GLOBECOM*, Anaheim, CA, Dec. 3-7, 2012, pp. 5392–5397.
- [37] T. Bai and R. W. Heath, "Coverage and rate analysis for millimeter-wave cellular networks," *IEEE Trans. Wireless Commun.*, vol. 14, no. 2, pp. 1100–1114, Feb. 2015.
- [38] S. Singh, M. N. Kulkarni, A. Ghosh, and J. G. Andrews, "Tractable model for rate in self-backhauled millimeter wave cellular networks," *IEEE J. Sel. Areas Commun.*, vol. 33, no. 10, pp. 2196–2211, Oct. 2015.
- [39] D. He, B. Ai, and K. Guan, et. al., "Channel measurement, simulation, and analysis for high-speed railway communications in 5G millimeter-wave band," *IEEE Trans. Intell. Transp. Syst.*, vol. 19, no. 10, pp. 3144–3158, Oct. 2018.
- [40] S. Y. Geng, J. Kivinen, X. W. Zhao, and P. Vainikainen, "Millimeter wave propagation channel characterization for short-range wireless communications," *IEEE Trans. Veh. Technol.*, vol. 58, no. 1, pp. 3–13, Jan. 2009.
- [41] P. Wang, G. Yu, and Z. Zhang, "On the secrecy capacity of fading wireless channel with multiple eavesdroppers," in *Proc. IEEE ISIT'07*, Nice, France, June 2007, pp. 1301–1305.
- [42] S. Tomic, M. Beko, and M. Tuba, "A linear estimator for network localization using integrated RSS and AOA measurements," *IEEE Signal Processing Letters*, vol. 26, no. 3, pp. 405–409, Mar. 2019.

- [43] J. Barros, and M. R. D. Rodrigues, "Secrecy capacity of wireless channels," in *Proc. IEEE ISIT'06*, Seattle, USA, Jul. 2006, pp. 356–360.
- [44] I. K. Son, S. Mao, M. X. Gong, and Y. Li, "On frame-based scheduling for directional mmWave WPANs," in *Proc. IEEE INFOCOM'12*, Orlando, FL, Mar. 2012, pp. 2149–2157.